Dry reforming in a dielectric barrier discharge reactor with non-uniform discharge gap : effects of metal rings on the discharge behavior and performance

Dry Reforming in a Dielectric Barrier Discharge Reactor with Non-uniform Discharge Gap: Effects of Metal Rings on the Discharge Behavior and Performance

Jinxin Wang[a,b], Kaimin Zhang[a], Vera Meynen[a]* and Annemie Bogaerts[b]*

[a]Laboratory of Adsorption and Catalysis, Department of Chemistry, University of Antwerp, Universiteitsplein 1, 2610 Wilrijk, Antwerp, Belgium
[b]Plasma Lab for Applications in Sustainability and Medicine - ANTwerp, Department of Chemistry, University of Antwerp, Universiteitsplein 1, 2610 Wilrijk, Antwerp, Belgium

*Email: vera.meynen@uantwerpen.be; annemie.bogaerts@uantwerpen.be

Abstract

The application of dielectric barrier discharge (DBD) plasma reactors is promising in various environmental and energy processes, but is limited by their low energy yield. In this study, we put a number of stainless steel rings over the inner electrode rod of the DBD reactor to change the local discharge gap and electric field, and we studied the dry reforming performance. At 50 W supplied power, the metal rings mostly have a negative impact on the performance, which we attribute to the non-uniform spatial distribution of the discharges caused by the rings. However, at 30 W supplied power, the energy yield is higher than at 50 W and the placement of the rings improves the performance of the reactor. More rings and with a larger cross-sectional diameter can further improve the performance. The reactor with 20 rings with a 3.2 mm cross-sectional diameter exhibits the best performance in this study. Compared to the reactor without rings, it increases the CO_2 conversion from 7% to 16 %, the CH_4 conversion from 12% to 23%, and the energy yield from 0.05 mmol/kJ supplied power to 0.1 mmol/kJ (0.19 mmol/kJ if calculated from the plasma power), respectively. The presence of the rings increases the local electric field, the displaced charge and the discharge fraction, and also makes the discharge more stable and with more uniform intensity. It also slightly improves the selectivity to syngas. The performance improvement observed by placing stainless steel rings in this study may also be applicable to other plasma-based processes.

Keywords: Dry reforming; Plasma-based process; Dielectric barrier discharge reactor; Non-uniform discharge gap; Energy yield improvement

1. Introduction

The application of plasma technology in chemical reactions is attractive and has been widely studied in a variety of processes, such as the decomposition of pollutants and synthesis of chemical products [1-3]. CO_2 reforming of CH_4 (dry reforming) is one of them. It can produce CO and H_2 (which could be used to produce clean fuels and chemicals) from renewable sources while reducing emissions of two greenhouse gases [4-7]. In the traditional thermal dry reforming, CH_4 and CO_2 need to be activated at a high temperature (at least 800 °C), resulting in problems of coking and energy losses [8]. Performing dry reforming in a plasma reactor can overcome these problems, because the high-energy electrons in non-equilibrium plasma are able to activate the molecules at relatively lower gas temperatures (lower than 250 °C) [9-14].

A common non-equilibrium plasma reactor is the dielectric barrier discharge (DBD) reactor, which is simple in design and can be operated at ambient temperature and pressure [5,15-17]. However, one of the main drawbacks of DBD reactors is their relatively low energy yield [8,18,19].

Khoja et al. studied the dry reforming of methane in DBD reactors with different dielectric materials and configurations, and a better energy yield of 0.085 mmol CO_2 and CH_4 converted per kJ plasma power was obtained for an alumina dielectric barrier [4]. Tu et al. [8] obtained an energy yield of 0.1 mmol/kJ in a DBD reactor combined with a catalyst, and this could be further improved to a maximum of 0.19 mmol/kJ by increasing the gas flow rate and reducing the specific energy input. Important to note that the energy yield in the above literature was calculated from the plasma power, and it could be about half to two-thirds of the value if it was calculated from the supplied power. The plasma discharge mode in a DBD reactor is mainly filamentary, and thus the plasma is not uniform in the whole space [20,21]. High-energy electrons exist almost exclusively in the discharge filaments [22,23]. The CH_4 and CO_2 molecules hit by the discharge filaments are dissociated upon electron collisions into various radicals, which can recombine into the products within the filaments or afterglow [23-25]. In addition to the dry reforming products, CO and H_2, some higher hydrocarbons can also be formed by radical recombination reactions [24,25]. The strength of the discharge filaments varies, which may result in poor product selectivity [26], and a too weak or too strong discharge causes energy waste, which may be one of the reasons for the lower energy yield of the DBD reactor [18,27].

Changing the design of the reactor is one method to improve the performance. DBD reactors with small discharge gaps (i.e., micro DBD reactors) may be able to increase the performance of dry reforming, due to the enhancement of the electric field [28,29]. Previous studies found that a reduced discharge gap did improve the conversion in DBD reactors at the same space time [30,31]. However, the same space time was maintained by reducing the gas flow rate, as the smaller gap reduced the discharge volume, and thus the energy yield of the conversion process is actually decreased.

In this study, we put a number of stainless steel rings with circular cross-sections over the stainless steel inner electrode rod of the reactor (see Fig. 1). These rings reduce the local discharge gap and change the electric field, which may promote the discharge with less effect on the discharge volume. This may induce the discharge to take place on the rings, which might change the discharge distribution and make the plasma more uniform, thereby changing the performance of the plasma-based dry reforming. Since the material of the rings is similar to that of the stainless steel inner electrode, and the rings cause a quite limited increase in the surface area of the inner electrode, the possible catalytic effect of the stainless steel rings is not considered in this study. In addition, in a plasma-based process with a catalyst, the metal active components on the catalyst surface will also be in contact with the electrodes and might have a similar effect, but the performance caused by the physical and chemical (surface) effects cannot be distinguished in a catalyst. Therefore, the role of the metal rings in this study can also provide a reference for the study of catalysts with metal components.

2. Experimental

2.1. Set-up for plasma-based dry reforming

A coaxial cylindrical DBD reactor was applied for plasma-based dry reforming. The original inner electrode was a smooth stainless steel rod with a diameter of 8 mm. A number of stainless steel rings with an inner diameter of 8 mm were put over the inner electrode at even intervals, as illustrated in Fig. 1. The cross-section of the rings is circular, and rings with two cross-sectional diameters, i.e., 1.6 mm and 3.2 mm, were used in this study.

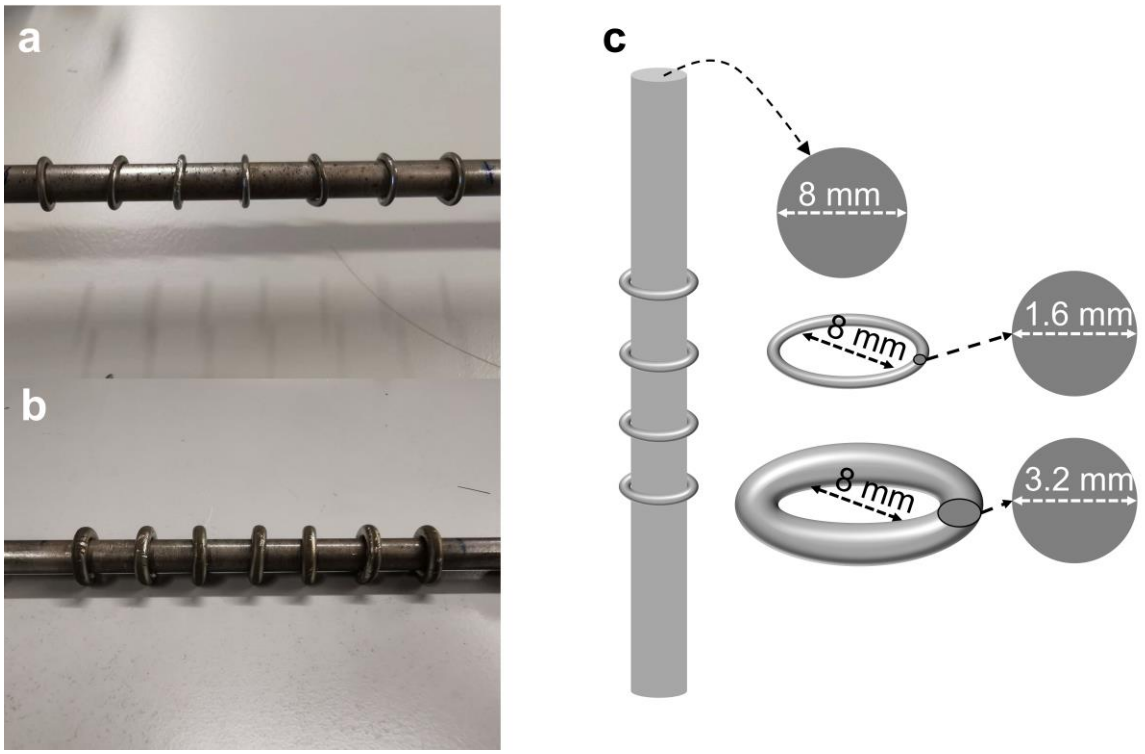

Fig. 1. Photographs of the stainless steel rod inner electrode, with stainless steel rings with cross-sectional diameters of (a) 1.6 mm and (b) 3.2 mm. (c) Schematic diagram of stainless steel rod, stainless steel rings and their dimensions.

Fig. 2 shows the whole set-up for the dry reforming experiments. The inner electrode was grounded. An alumina tube with an inner diameter of 17.4 mm and an outer diameter of 21.8 mm was coaxially placed over the inner electrode as a dielectric barrier, so the discharge gap of the ring-free reactor, which is the spacing between the 8 mm inner electrode and dielectric barrier, was about 4.7 mm. A stainless steel mesh tightly wound around the dielectric barrier tube was used as the external electrode. It was connected to high voltage supplied by a function generator (Tektronix, AFG 2021) and a high voltage amplifier (TREK, model 20/20C-HS). The length of the outer electrode was 100 mm, which defined the discharge length. According to the parameters of the reactor, the volume of the discharge zone was calculated to be 18.8 mL. A sinusoidal alternating input signal with a frequency of 3 kHz was provided by the function generator, and was then amplified by the amplifier. The voltage was measured by a high-voltage probe (Tektronix, P6015A), and the current was monitored by a Rogowski coil (Pearson 4100). A capacitor (10 nF) and a low-voltage probe (Picotech, TA150) connected in parallel with it were connected in series with the reactor to monitor the charge. The oscilloscope and connected PC collected and displayed all the electrical signals to calculate the power in real time. The power of the power supply was kept constant by adjusting the amplitude of the input signal from the amplifier according to the calculated power on the PC.

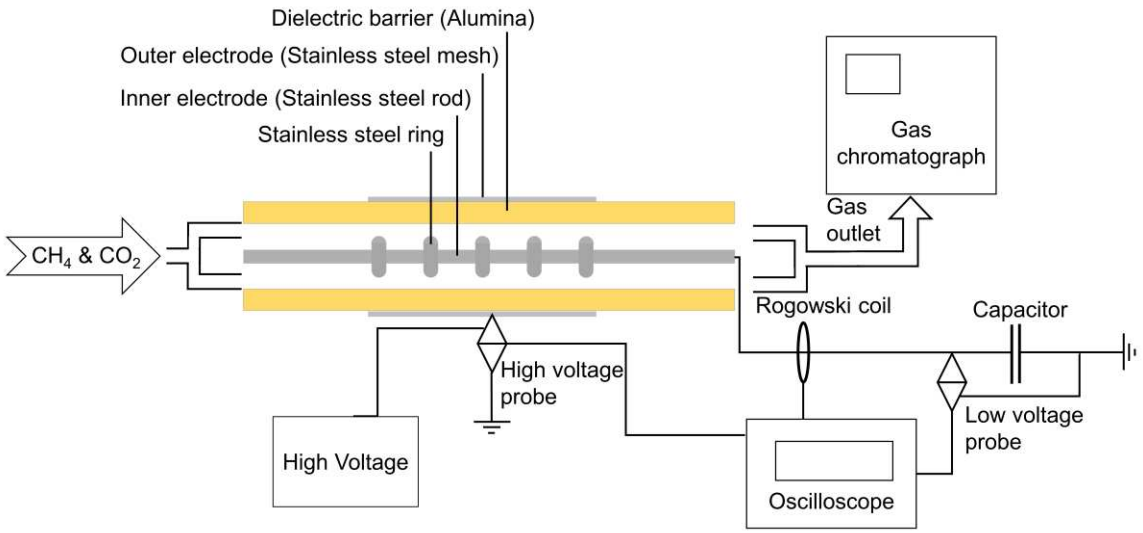

Fig. 2. DBD plasma set-up and analytical system for the dry reforming experiments.

2.2. Performance of plasma-based dry reforming

The feed gas into the reactor was composed of 10 mL/min of CH_4 and 10 mL/min of CO_2 controlled by mass flow controllers (Bronkhorst EL-FLOW Select). Since the produced CO, H_2 and unknown amounts of various (oxygenated) hydrocarbons by the dry reforming reaction causes an unknown expansion coefficient and thus a possible pressure increase, while the GC always samples at a constant ambient pressure, the outlet gas composition analyzed by the GC would have systematic errors. Therefore, an internal standard gas, 10 mL/min of N_2, was added into the outlet gas to exclude these errors [32]. An online gas chromatograph (Trace GC 1310, Interscience) with a thermal conductivity detector (TCD) and a flame ionization detector (FID) was applied to analyze the composition and concentration of the outlet gas. The composition of the gas after the gas circuit was flushed for 30 minutes and before turning on the plasma, was denoted as $CO_{2,in}$ and $CH_{4,in,}$. The power was then turned on to generate plasma and maintained at a constant supplied power for 30 min. The outlet gases were analyzed and denoted with "out", i.e., $CO_{2,out}$, $CH_{4,out}$, CO_{out}, $H_{2,out}$ and $C_xH_yO_{z,out}$. The conversion of CO_2 and CH_4 were calculated by Eq. (1) and Eq. (2):

$$X_{CO_2}(\%) = \frac{CO_{2,in} - CO_{2,out}}{CO_{2,in}} \times 100\% \quad (1)$$

$$X_{CH_4}(\%) = \frac{CH_{4,in} - CH_{4,out}}{CH_{4,in}} \times 100\% \quad (2)$$

The (H-based) selectivity of H_2, and the C-based selectivity of CO and of the other chemicals were defined by Eq. (3) to Eq. (5):

$$S_{H_2}(\%) = \frac{H_{2,out}}{2 \times (CH_{4,in} - CH_{4,out})} \times 100\% \quad (3)$$

$$S_{CO}(\%) = \frac{CO_{out}}{(CH_{4,in} - CH_{4,out}) + (CO_{2,in} - CO_{2,out})} \times 100\% \quad (4)$$

$$S_{C_xH_yO_z}(\%) = \frac{x \times C_xH_yO_{z,out}}{(CH_{4,in} - CH_{4,out}) + (CO_{2,in} - CO_{2,out})} \times 100\% \quad (5)$$

In this study, the energy yield (EY) of dry reforming was defined as the mmol of CO_2 and CH_4 that can be converted per kJ of supplied energy, as shown in Eq. (6):

$$\mathrm{EY}\left(\frac{\mathrm{mmol}}{\mathrm{kJ}}\right) = \frac{V_{CO_2}X_{CO_2}+V_{CH_4}X_{CO_4}}{P_{sply}V_m} \times \frac{1000}{60}\left(\frac{\mathrm{Wmin}}{\mathrm{kJ}}\right) \quad (6)$$

Where V_{CO2} and V_{CH4} were the volumetric flow rate of CO_2 and CH_4 in the feed gas, respectively (in mL/min), and X_{CO2} and X_{CH4} are the conversion of CO_2 and CH_4, respectively. V_m is the molar gas volume (24.4 mL/mmol). It should be noted that P_{sply} in Eq. 6 is the supplied power (in W), and not the discharge power as used in most literature [8,33]. Indeed, we also want to include the effect of the reactor on the discharge power in the calculation of the energy yield. If the discharge power is used to calculate the EY, we will get a larger value, about 1.5–2 times larger, than the EY presented in this paper.

2.3. Electrical characterization

To better understand the effect of adding the stainless steel rings on the reaction performance, we performed an electrical characterization of the plasma. The above-mentioned high voltage probe, low voltage probe, Rogowski coil and capacitor in the plasma set-up can collect the data of the voltage, current and charge during the discharge. Errors were obtained from three repeat experiments. The discharge power was calculated by voltage U and current I, via Eq. (7):

$$P_{sply}(W) = \int_0^T UI\,dt \quad (7)$$

A Q-U graph, known as a Lissajous figure, was plotted using the voltage and charge data. Fig. 3 shows a typical Lissajous figure of the plasma in a DBD reactor. The slopes of the sides of the Lissajous figure represent the equivalent capacitance of the DBD reactor at different phases, since dQ/dU = C. The slopes of the Lissajous figures (dQ/dU) in this work were calculated by a Matlab script [30]. In the AB and CD phases when the reactor is not discharged, the entire DBD reactor, including the dielectric barrier and discharge gap, behaves as a capacitor. Therefore, the slope of the AB and CD phases in the Lissajous figure is the capacitance of the capacitor formed by the dielectric barrier and the discharge gap in series, denoted by C_{cell}. Plasma occurs in the BC and DA phases. During the discharge, a part of the discharge gap behaves like a resistor due to the breakdown of the reactive gas, while the dielectric barrier and another part of the discharge gap (because the entire gap is not fully discharged in a DBD reactor) still behave as a capacitor. Therefore, the slope of the BC and DA phases, denoted by ζ, represents the capacitance including the dielectric barrier and the undischarged gap.

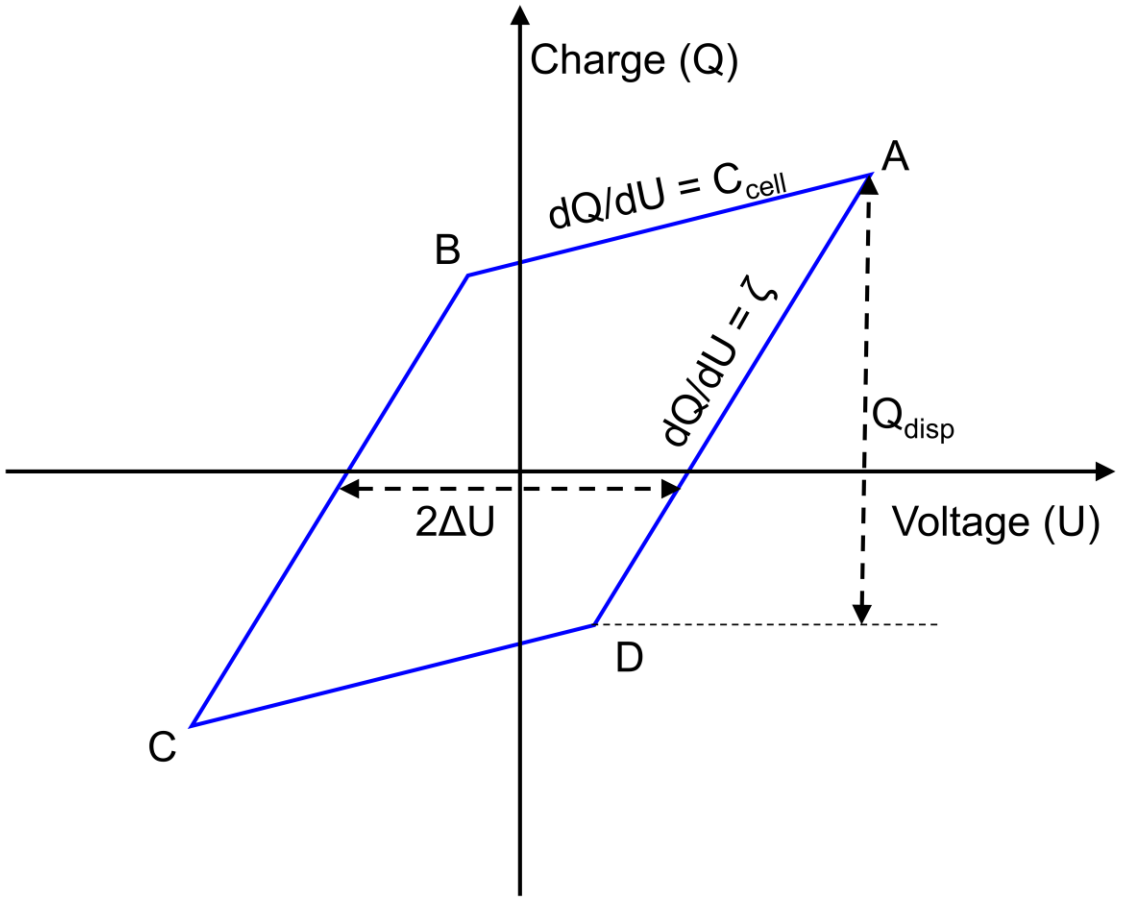

Fig. 3. Typical Lissajous figure of a discharge in a DBD reactor.

The capacitance C_{diel} of the dielectric barrier alumina tube, used in this work, is 0.266 nF, which was measured in a previous study [30]. Using C_{cell}, ζ and C_{diel}, the discharging areal fraction, denoted as f, of the DBD reactor was calculated by Eq. 8 [34].

$$f = \frac{\zeta - C_{cell}}{C_{diel} - C_{cell}} \quad (8)$$

The burning voltage (U_{bur}) of the plasma in the reactor was calculated from C_{cell}, ζ, C_{diel} and the voltage at Q = 0 C in the Lissajous figures, i.e., ΔU, by Eq. 9 [34].

$$U_{bur} = \frac{1 - C_{cell}/C_{diel}}{1 - C_{cell}/\zeta} \Delta U \quad (9)$$

The mean electric field (E) in the reactors was calculated by the following equation [35]:

$$E = \frac{U_{bur}}{d_{gap}} \quad (10)$$

Where d_{gap} is the discharge gap, which is 4.7 mm in the reactor without rings. The electric field for the reactor with rings, as calculated in this study, was the mean electric field between the rings and the dielectric barrier, as we believe the discharge mainly takes place on the rings. The value of d_{gap} in the reactor with rings is 3.1 mm and 1.5 mm, respectively, for the rings with thickness of 1.6

mm and 3.2 mm. It should be noted that this mean electric field is only an approximation, because in reality the potential will not drop linearly between the inner electrode (or the rings) and the outer dielectric barrier, so the electric field will also not be constant, but it will be larger in the sheath near the inner electrode (or rings). However, as we cannot measure the exact electric field distribution inside the reactor, the above equation (10) is only an averaged estimate. Subsequently, the mean electron energy and electron energy distribution function (EEDF) were calculated from the mean electric field, by the Boltzmann equation using BOLSIG+ [36].

The charge difference between the points A and D in the Lissajous figure was the displaced charge in the DA discharge phase. It was divided by the number of micro-discharges counted in the current profile to get the average intensity of discharge filaments [30].

3. Results and discussion

The plasma-based dry reforming performance in a DBD reactor, with stainless steel rings over the inner electrode, was tested at 50 W and 30 W supplied power.

3.1. Plasma-based dry reforming at 50 W supplied power

3.1.1. Conversion and energy yield

Fig. 4 illustrates the influence of placing stainless steel rings over the inner electrode rod on the CH_4 and CO_2 conversions and on the energy yield of plasma-based dry reforming at 50 W supplied power, for the rings with a cross-sectional diameter of 1.6 mm and 3.2 mm. A difference in performance for the reactors with and without rings was observed, and also the number of rings had an effect. Since the supplied power could not be controlled precisely at 50 W all the time (see Table 1), sometimes changes in CH_4 and CO_2 conversions could not correctly reflect changes in reactor performance. The energy yield can reflect a more accurate trend of the performance. Since all experiments were performed at the same gas flow rate, and not the same space time, the specific input energy (SEI) was only related to the power, and the energy yield follows a similar trend as the conversion. As shown in Fig. 4a, for 1.6 mm rings, the energy yield and the reactant conversions increase with the number of rings. However, they were always lower than in the reactor without rings. The rings with a cross-sectional diameter of 3.2 mm (Fig. 4b) showed better performance and a similar but more pronounced increasing trend upon placing more rings. The reactors with only a few rings also had lower performance than the reactor without rings. However, the CO_2 conversion of the reactors with more than 10 rings exceeded that of the reactor with no rings, and the reactor with more than 15 rings also showed a higher energy yield. The DBD reactor with 20 rings with 3.2 mm cross-sectional diameter exhibited the best performance, although the improvement compared with the reactor without rings was limited.

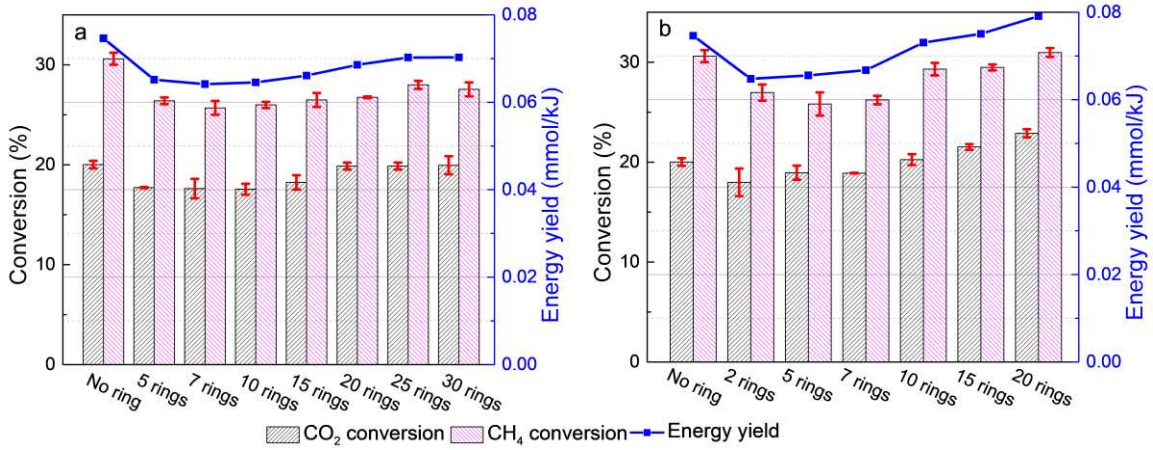

Fig. 4. CH_4 and CO_2 conversion and energy yield of plasma-based dry reforming at 50 W supplied power, in a DBD reactor without rings, and with a varying number of stainless steel rings placed over the inner electrode, with cross-sectional diameters of (a) 1.6 mm and (b) 3.2 mm. The error bars were obtained from standard errors based on three repeat experiments with the rings kept in place.

Placing stainless steel rings over the inner electrode mainly has the following effects on the discharge in the DBD reactor. First of all, as introduced in the experimental section, the discharge gap between the inner electrode and the dielectric barrier was 4.7 mm (i.e., 17.4 mm − 8 mm, divided by 2). The metal rings reduced the discharge gaps at this location, to values of 3.1 mm and 1.5 mm, for the 1.6 mm and 3.2 mm rings, respectively (i.e., 17.4 mm – 11.2 mm, divided by 2; and 17.4 mm – 14.4 mm, divided by 2). The reduction in discharge gap causes a higher reduced electric field strength and power density at the metal rings, leading to more displaced charge per period (see section 3.1.2 below) and a higher electron energy. Therefore, more gas molecules can be hit by the discharge filaments [37], and more successful electron impact excitation can occur in the plasma [38]. These are the positive effects of the metal rings on the plasma behavior, which should increase the performance of the reactor [39]. The 3.2 mm rings exhibit better performance than the 1.6 mm rings due to the smaller discharge gap. However, these positive effects are not well reflected between reactors with and without rings in Fig. 4, indicating the presence of negative effects, resulting in the majority of the ring-based configurations at 50 W supplied power being lower in performance than for the reactor without rings.

Second, the presence of rings in the discharge space of the DBD reactor occupies the available discharge volume. Since the same gas flow rate was applied in the experiments in Fig. 4, the discharge volume reduction reduced the space time of plasma-based dry reforming. This is unfavorable to the conversion of CH_4 and CO_2. In previous studies on a micro-gap DBD reactor [30], the reduction in discharge volume resulted in a lower energy yield than reactors with larger discharge gaps, despite the stronger electric field in the micro-gap reactor. However, the metal rings in this study only occupy part of the discharge volume at the location where the rings were placed, which is much smaller than the drop in volume brought by reducing the entire discharge gap in the micro-gap reactors. Moreover, as observed in Fig. 4, increasing the number or the cross-sectional diameter of the rings causes some improvement in conversion and energy yield (even when compared to the reactor without rings in some cases), although more rings means a larger discharge volume reduction. This suggests that although metal rings do reduce the discharge volume to some extent (~0.05 mL for each 1.6 mm ring and ~0.2 mL for each 3.2 mm ring), this is not the main negative factor that leads to the lower performance of the reactor with rings than the reactor without rings.

Finally, compared with the smooth and uniform surface of the inner electrode rod, discharges are more likely to take place on the metal rings with stronger reduced electric fields. This makes the discharge more stable and more uniform in intensity (see section 3.1.2 below), which may be beneficial to reduce the formation of by-products and improve the selectivity of the desired products [26]. However, the spatial distribution of the discharges becomes relatively non-uniform, as it is more difficult for the discharge to take place where no metal rings are present. The place where the discharge can take place on the inner electrode has changed from the 10 cm long electrode rod to probably only the top of a few rings, so the volume of the discharge space is expected to be greatly reduced. This reduces the chance of gas molecules being hit by the discharges, resulting in an expected reduced conversion and energy yield [37]. Increasing the number of rings will reduce the distance between the rings, and is thus expected to improve the spatial uniformity of the plasma, in line with the trend in Fig. 4 that the performance increases with the number of rings. This indicates that the non-uniform spatial distribution of the discharge is a more dominant negative effect of the stainless steel rings on the reactor performance compared to the volume occupied by the metal rings. The negative effects play a more dominant role at 50 W, making the reactor with rings to perform worse in most cases than the original reactor without rings.

3.1.2. Electrical characterization

Electrical characterization data of the above experiments were collected and calculated to better understand the effect of the stainless steel rings. The data that can be obtained directly from the raw measurement data or through simple calculations like averaging, are listed in Table 1. In most cases, the required applied voltage (presented in Table 1 as the root mean square voltage V_{RMS}) to achieve a 50 W supplied power in the reactors with rings was smaller than in the reactor without rings. Moreover, the required V_{RMS} decreased with the number of rings, while the root mean square current (I_{RMS}) of the generated plasma increased. Stronger plasma currents (higher I_{RMS} values) indicate stronger or more discharges induced by the rings in the reactor, possibly promoting the production of active species, i.e., electrons, ions and radicals. In addition, the presence of the rings enhanced the local electric field, making the discharge easier to take place in the reactor, so that a certain power could be achieved at a lower applied voltage. Reactors with fewer than 15 rings with 1.6 mm diameter had a lower I_{RMS} than the ring-free reactor, due to the limited promotion induced by the thinner rings on the discharge and because the discharge can only occur on fewer rings, while reactors with more than 15 rings with 1.6 mm diameter and all reactors with 3.2 mm rings had a higher I_{RMS} than the ring-free reactor, thus indicating stronger and more discharges, that can promote the formation of active species, as mentioned above. The V_{RMS} trend of the reactors with 1.6 mm rings was not obvious when the number of rings was above 10. For the 3.2 mm rings, the V_{RMS} was lower and the I_{RMS} was higher than for the same number of 1.6 mm rings, and the decrease in V_{RMS} with the number of rings was more pronounced. The plasma power of the 1.6 mm rings did not show a clear trend, while the 3.2 mm rings showed a trend of decreasing plasma power with increasing number of rings, which is, in principle, negative to the performance of the reactor.

Table 1. Measured data from the input signals of the oscilloscope, including voltage, current, charge and power, for the DBD reactors without rings, and with stainless steel rings of varying number and two different cross-sectional diameters, at an almost constant supplied power of 50 W.

Cross-sectional diameter of rings	Number of rings	V_{RMS} (kV)	I_{RMS} plasma (mA)	Plasma power (W)	Supplied power (W)	Displaced charge (nC/period)
Without rings	0	7.03 ± 0.04	19.5 ± 0.7	31.3 ± 0.8	51 ± 1	980 ± 35
1.6 mm	5	6.86 ± 0.04	16.8 ± 0.4	32 ± 1	50.4 ± 0.8	1150 ± 29
	7	6.54 ± 0.04	18.3 ± 0.5	32.2 ± 0.5	50.2 ± 0.5	1210 ± 15
	10	6.26 ± 0.02	18.8 ± 0.2	32.7 ± 0.1	50.2 ± 0.1	1260 ± 19
	15	6.04 ± 0.04	19.7 ± 0.4	32.7 ± 0.6	50.3 ± 0.5	1320 ± 24
	20	6.09 ± 0.02	21.8 ± 0.9	33 ± 1	50.6 ± 0.4	1314 ± 8
	25	6.08 ± 0.04	22.1 ± 0.2	32.3 ± 0.6	50.7 ± 0.5	1320 ± 12
	30	6.15 ± 0.07	22.4 ± 0.2	31.9 ± 0.3	50.3 ± 0.6	1290 ± 13
3.2 mm	2	7.14 ± 0.04	20.0 ± 0.3	30.8 ± 0.9	51.6 ± 0.9	1070 ± 16
	5	6.79 ± 0.04	21.4 ± 0.3	29.0 ± 0.2	51.1 ± 0.3	1320 ± 15
	7	6.44 ± 0.03	22.6 ± 0.3	28.5 ± 0.7	50.3 ± 0.7	1420 ± 6
	10	6.15 ± 0.04	24.5 ± 0.9	28.1 ± 0.5	50.5 ± 0.5	1498 ± 6
	15	5.90 ± 0.04	25.1 ± 0.4	27.9 ± 0.2	50.5 ± 0.6	1600 ± 11
	20	5.89 ± 0.01	24.9 ± 0.9	26.7 ± 0.6	50.6 ± 0.2	1652 ± 7

Fig. 5 shows the fitted Lissajous figures (consisting of the calculated slopes) of the plasma at 50 W supplied power, in reactors with varying number and two different cross-sectional diameter of the stainless steel rings. The raw data of the Lissajous figures are shown in Fig. S1, in the supporting information. Obvious differences can be observed from the Lissajous figures. First of all, the height of the Lissajous figure of the reactors with rings is higher than that of the reactor without rings, and it continues to increase as the number of rings increases. This indicates that the metal rings lead to more charge displacement within the plasma, which supports the aforementioned discharge promotion by the enhanced reduced electric field. The specific values of the displaced charges were calculated by taking the charge difference between points A and D of the Lissajous figures, and are listed in Table 1. For the 1.6 mm rings, only the reactors with less than 15 rings showed an obvious trend of increasing the displaced charge with increasing number of metal rings, while the trend for the 3.2 mm rings is still relatively obvious until the maximum of 20 rings. Furthermore, the displaced charge in case of the 3.2 mm rings was always more than that of the 1.6 mm rings with the same number of rings, which should be one of the reasons why the reactors with 3.2 mm rings showed higher performance.

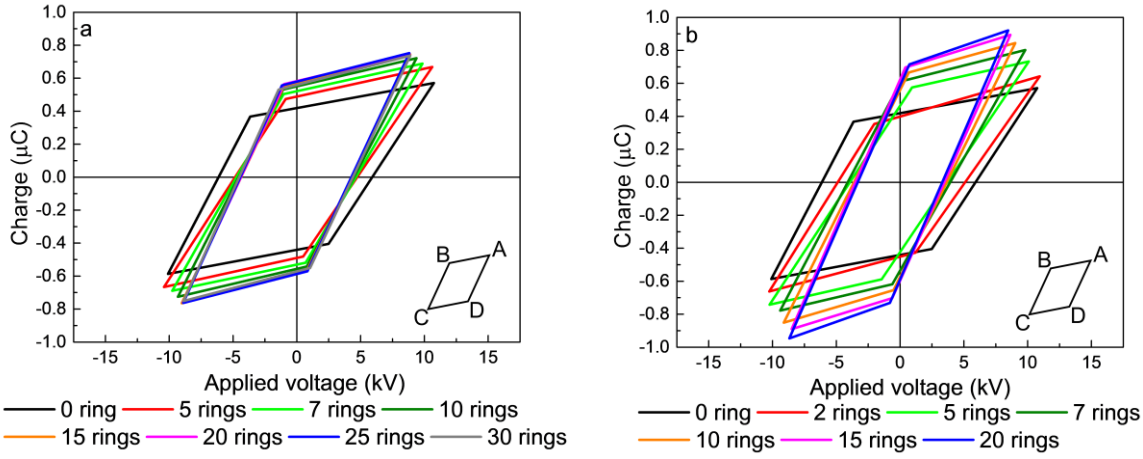

Fig. 5. The fitted Lissajous figures (calculated by the MATLAB script) of plasma-based dry reforming at 50 W supplied power, in a DBD reactor without rings, and with varying number of stainless steel rings with cross-sectional diameters of (a) 1.6 mm and (b) 3.2 mm.

Second, the voltage at Q = 0 C in the Lissajous figures, which is related to the burning voltage (U_{bur}) of the plasma in the reactor, was changed by the rings. As shown in Table 2, after placing the stainless steel rings on the inner electrode, U_{bur} was significantly reduced. Furthermore, as the number of rings increases, U_{bur} shows a roughly decreasing trend. This suggests that the metal rings made it easier to ignite and sustain the plasma at relatively lower voltages. Moreover, the 3.2 mm rings lower the U_{bur} more than the 1.6 mm rings. The mean electric field can be calculated from U_{bur} and the discharge gaps, and it is increased by the presence of the rings, due to the reduced discharge gap. It should be noted that the electric field shown in Table 2 is the mean electric field at the position of the rings (calculated from the gap between the rings and the dielectric barrier) in the reactor with rings, as we believe that the discharge mainly take place on the rings. The electric field decreases as the number of rings increases, due to the lower burning voltage of the plasma in the reactor with more rings. The mean electron energy and electron energy distribution function (EEDF) are also shown in Table 2 and Fig. S2, respectively. The metal rings enhance the mean electron energy in the reactor, however, this electron energy is too high for efficient vibrational excitation of CO_2 in plasma-based dry reforming [18,27]. As vibrational excitation is the most energy-efficient pathway for dissociation, this might be one of the reasons why the performance of the reactor with rings at 50 W is lower than the original reactor without rings. Similar with the trend of the electric field, the mean electron energy also decreases with increasing number of rings, which may be one of the reasons for the enhancement in reactor performance with increasing number of rings. However, due to other physical changes that cause positive effects of the rings on the discharge (as described above and below), the reactor with 3.2 mm rings performed better than the reactor with 1.6 mm rings despite the higher mean electron energy. Even, some reactors (with more than 15 rings) performed better than the reactor without rings at 50 W.

Finally, the slope of each side of the Lissajous figures also changes, indicating that the metal rings change the capacitance of the DBD reactor. The slope (capacitance of the entire reactor) C_{cell} of the undischarged phases and the slope ζ representative for the capacitance of the discharged phases are listed in Table 2. The capacitance C_{cell} of all the reactors with rings is always higher than that of the reactor without rings, because the discharge gaps are reduced by placing the metal rings. There seems to be a slightly rising trend of C_{cell} with the number of rings, but some cases do not follow it. On the other hand, ζ, has a clearly increasing trend with the number of rings. Since the DBD reactor was not fully discharged, the capacitance represented by ζ includes the capacitance of the undischarged gap and the dielectric barrier. The capacitance of the dielectric barrier is constant because the same barrier was used in all experiments. Therefore, the rise of ζ indicates that the undischarged fraction decreases upon increasing number of rings. The fractions of discharges (denoted by f) in the reactors, calculated from C_{cell} and ζ, are also listed in Table 2. For the 1.6 mm rings, the discharge fraction increases from 40.0% for 5 rings to 60.1% for 30 rings, while for the 3.2 mm rings, it increases from 38.7% for 2 rings to 62.9% for 20 rings, hence showing a larger increase rate. Since the gas flow rate was approximately constant and the plasma power was even reduced (at a constant supplied power) with the number of rings, the larger discharge fraction by the stainless steel rings was achieved without increasing the specific energy input. It needs to be noted that the plasma discharge fraction of the reactors with 5 rings or less, both for the 1.6 mm and 3.2 mm rings, was smaller than that of the reactor without rings, but as the number of rings increases, the discharge fraction becomes larger than in the reactor without rings. This is in line with the effect mentioned above: the metal rings can promote the discharge but will induce the discharge mainly taking place on the rings, resulting in a non-uniform spatial distribution of the discharge. The spacing between the rings, where it is more difficult for the discharge to take place, is large in reactors with fewer than five rings, and hence in this case the discharge fraction is even smaller than that of a reactor without rings. As the number of rings increases, the negative effect on the discharge fraction decreases and the positive effect increases, so the discharge fraction increases substantially.

Table 2. Calculated data derived from the raw data of electrical characterization, obtained by a MATLAB script and BOLSIG+, for the DBD reactors without rings and with stainless steel rings of varying number and two different cross-sectional diameters, at an almost constant supplied power of 50 W.

Cross-sectional diameter of rings	Number of rings	U_{bur} (kV)	Electric field (kV/cm)	Mean electron energy (eV)	C_{cell} (pF)	ζ (pF)	f (%)	Number of micro-discharges (a.u./T)	Average filament charge (nC/disch.)
Without rings	0	6.3 ± 0.1	12.8 ± 0.2	3.31 ± 0.06	14.3 ± 0.5	133.1 ± 0.3	47.2 ± 0.2	90 ± 22	11 ± 3
1.6 mm	5	5.2 ± 0.1	15.7 ± 0.3	3.75 ± 0.06	16.9 ± 0.4	116.5 ± 0.5	40.0 ± 0.3	75 ± 2	15 ± 1
	7	5.0 ± 0.1	15.1 ± 0.3	3.67 ± 0.06	16.6 ± 0.3	134.3 ± 0.7	47.2 ± 0.3	80 ± 5	15 ± 2
	10	4.7 ± 0.2	14.2 ± 0.6	3.53 ± 0.07	18.2 ± 0.3	149.7 ± 0.3	53.1 ± 0.1	81 ± 3	16 ± 1
	15	4.5 ± 0.2	13.6 ± 0.6	3.44 ± 0.07	19.5 ± 0.6	162.9 ± 0.2	58.2 ± 0.3	81 ± 7	16 ± 1
	20	4.5 ± 0.1	13.6 ± 0.3	3.44 ± 0.06	18.8 ± 0.3	165.7 ± 0.4	59.4 ± 0.2	96 ± 9	14 ± 1
	25	4.48 ± 0.03	13.5 ± 0.1	3.43 ± 0.06	19.7 ± 0.8	168.0 ± 0.7	60.2 ± 0.1	83 ± 7	16 ± 2
	30	4.6 ± 0.1	13.9 ± 0.3	3.48 ± 0.06	20.1 ± 0.5	167.8 ± 0.6	60.1 ± 0.2	93 ± 9	14 ± 1
3.2 mm	2	5.7 ± 0.3	33.3 ± 1.8	5.4 ± 0.2	21.4 ± 0.7	116.0 ± 0.5	38.7 ± 0.2	140 ± 11	8 ± 2
	5	4.1 ± 0.1	23.9 ± 0.6	4.65 ± 0.07	17.3 ± 0.5	116.2 ± 0.9	39.8 ± 0.2	126 ± 5	10 ± 1
	7	4.2 ± 0.2	24.5 ± 1.2	4.7 ± 0.1	18.9 ± 0.4	141.6 ± 0.4	49.7 ± 0.3	163 ± 4	9 ± 2
	10	3.9 ± 0.1	22.8 ± 0.6	4.54 ± 0.07	22.2 ± 0.9	155.9 ± 0.7	54.8 ± 0.4	150 ± 6	10 ± 3
	15	3.7 ± 0.2	21.6 ± 1.2	4.4 ± 0.1	24 ± 1	175.2 ± 0.5	62.5 ± 0.4	165 ± 4	10 ± 1
	20	3.5 ± 0.1	20.4 ± 0.6	4.31 ± 0.07	27.0 ± 0.3	177.4 ± 0.7	62.9 ± 0.3	135 ± 4	12± 1

Fig. 6 shows the current profiles in the DBD reactors with varying number and two different cross-sectional diameters of the stainless steel rings. Comparing the reactors without and with fewer rings (≤ 5), the current intensity is more uniform in the reactor with rings, and the uniformity increases with the number of rings. The difference in current profiles between the reactors with relatively more rings is not significant, but it seems that the uniformity of current intensity slightly decreases with increasing number of rings, see for example the reactors with 5 and 20 rings with a diameter of 3.2 mm. This confirms that the rings can make the discharge more uniform in intensity, which may change the selectivity of some products. The discharge onset in the reactors with rings is earlier, which is consistent with one of the conclusions of Fig. 5 that the rings reduce the burning voltage of the plasma. The number of peaks in the current profiles is a measure for the number of micro-discharges in the plasma, this number is also listed in Table 2. The number of micro-discharges in the reactors with 1.6 mm rings is similar to that in the reactor without rings, while the number of micro-discharges in the reactor with the 3.2 mm rings is clearly higher (cf. Table 2).

Finally, the average filament charge of the micro-discharges can be obtained by dividing the displaced charge by the number of micro-discharges, and is a measure of the average discharge intensity. The average filament charge in case of the 1.6 mm rings is higher than that of the reactor without rings, while that of the 3.2 mm rings is similar to or even lower. Metal rings with both cross-sectional diameters improve the displaced charge within the plasma, as mentioned above, but the improvement for the 1.6 mm rings is on the average filament charge, or average discharge intensity, while the improvement for the 3.2 mm rings is on the number of micro-discharges. Hence, the change in discharge behavior caused by the stainless steel rings is different, possibly depending on the size of the remaining discharge gap between the metal and the dielectric barrier. Although the above electrical characterizations show a lot of positive effects of the rings, they are not sufficient to compensate for the negative effects of the non-uniform spatial distribution of the discharge and the high electron energy. The reactors with rings showed in most cases a worse performance than the reactor without rings. Only when having more rings (≥ 15) with a diameter of 3.2 mm, the reactor with rings performed better than the reactor without rings, due to its greater improvement on the discharge and less negative impact of the non-uniform discharge spatial distribution and the high electron energy.

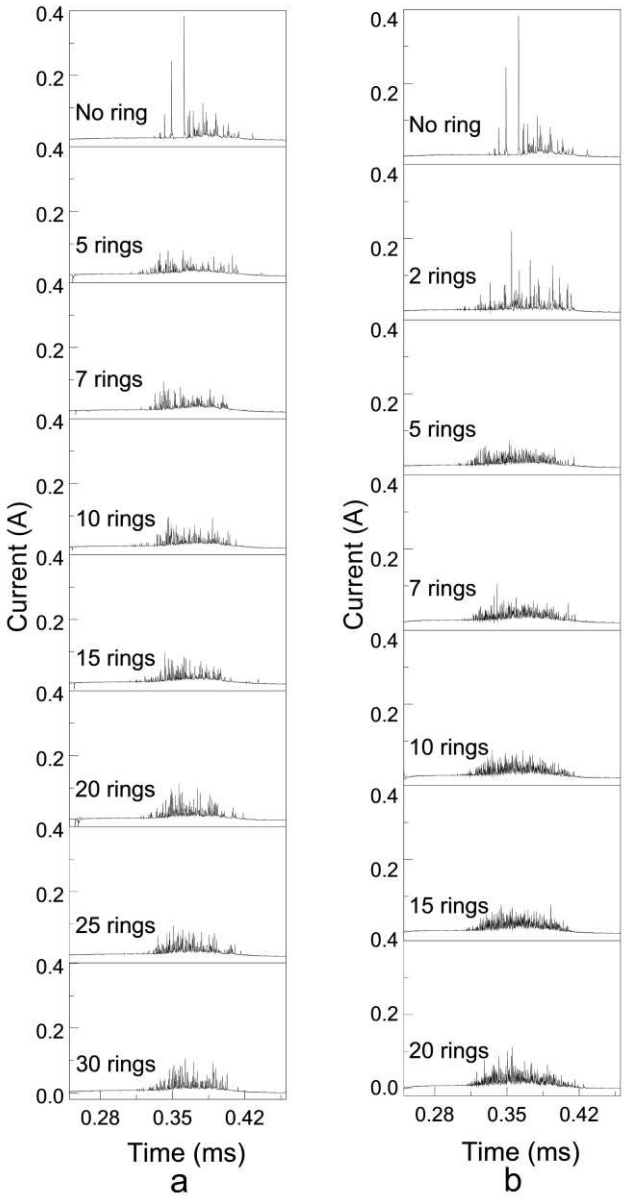

Fig. 6. Current profiles of a discharge phase in DBD reactors at 50 W supplied power, without rings, and with a varying number of stainless steel rings with cross-sectional diameters of (a) 1.6 mm and (b) 3.2 mm.

3.1.3. Selectivity

Due to the limited surface area of the rings and the fact that a similar material was used as for the stainless steel inner electrode, we believe that the conversion and selectivity changes are mainly caused by the physical effect of the rings on the discharge. Fig. 7 shows the selectivity of various products in the DBD reactor without rings and with varying numbers of stainless steel rings at 50 W supplied power, for both 1.6 mm and 3.2 mm rings. Not only syngas is formed, but also other products, such as various hydrocarbons and oxygenations are formed in the DBD reactor, among others by radical recombination [24,25]. It needs to be noted that some possible liquid products (e.g., oily hydrocarbons, alcohols) and carbon deposits attached to the reactor, as well as other gaseous products not calibrated in the gas chromatograph, cannot be counted, and therefore, the carbon and hydrogen mass balance calculated from the product selectivity does not reach 100% (as

shown in Fig. S3 of the Supporting Information). As is clear from Fig. 7, at 50 W supplied power, the placement of the metal rings and the number of rings only had a small effect on the selectivity of most products. The exception is that there is a slightly increasing trend for the selectivity of methanol with the number of rings, and the selectivity of ethane is more affected, although without a clear trend.

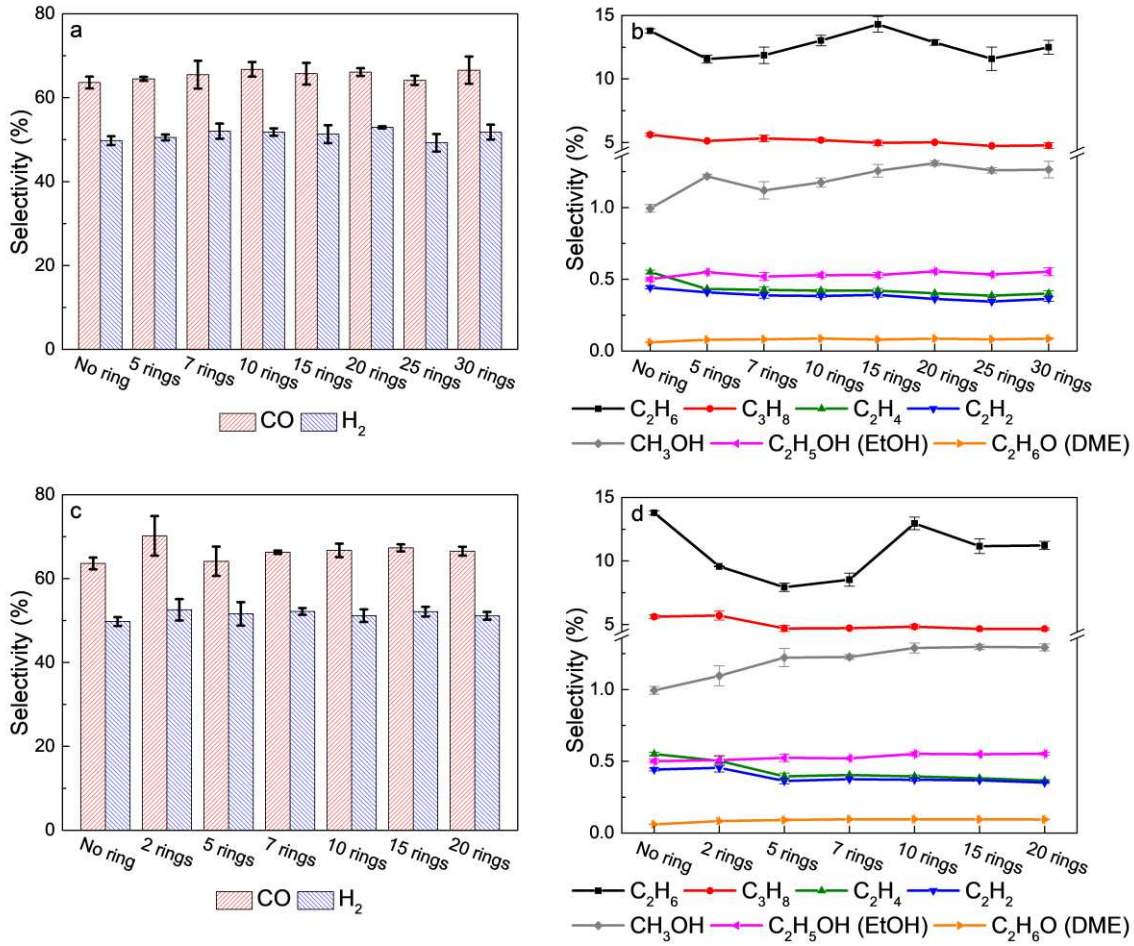

Fig. 7. Selectivity of various products of plasma-based dry reforming at 50 W supplied power, in a DBD reactor without rings, and with varying number of stainless steel rings. (a) Syngas and (b) ethane, propane, ethylene, acetylene, methanol, ethanol (EtOH) and dimethyl ether (DME) selectivity in reactors with rings with a diameter of 1.6 mm. (c) Syngas and (d) ethane, propane, ethylene, acetylene, methanol, ethanol and dimethyl ether selectivity in reactors with rings with a diameter of 3.2 mm. The error bars were obtained from standard errors based on three repeat experiments with the rings kept in place.

3.2. Plasma-based dry reforming at 30 W supplied power

3.2.1. Conversion and energy yield

Fig. 8 shows the influence of the same 1.6 mm and 3.2 mm rings on the CH_4 and CO_2 conversions and the energy yield of plasma-based dry reforming, but at 30 W supplied power. The effect of the rings is clearly different from the case at 50 W. At 30 W, the energy yields and reactant conversions in all reactors with the rings are higher than in the reactor without rings. There is also a clear effect of the number of rings to the conversion and energy yield, and the performance of the reactor with 3.2 mm rings has a tendency to increase with the number of rings. Compared with the reactor without rings, the increase of reactor performance resulting from the rings at 30 W supplied

power is much greater than at 50 W. The DBD reactor with 20 rings with a 3.2 mm cross-sectional diameter has the best performance, with an energy yield double the value of the reactor without rings. It enhances the CO_2 conversion from 7.1% to 16.3 %, the CH_4 conversion from 11.9% to 22.5%, and the energy yield from 0.05 mmol/kJ to 0.1 mmol/kJ. As already mentioned above, the energy yield in this work was calculated from the supplied power, and the energy yield of the reactor with the best performance is 0.19 mmol/kJ if calculated from the plasma power as in most of the literature. Furthermore, compared to the reactors with the same number and diameter of rings at a supplied power of 50 W, although the CO_2 and CH_4 conversions are reduced due to the lower power, the energy yield is actually improved by 17% on average at 30 W, except for the reactor without rings. The best performing reactor in this study, i.e., the one with 20 rings of 3.2 mm diameter, was investigated for its performance stability. As shown in Fig. S4, the conversion of CO_2 and CH_4 in this reactor did not change significantly during the 12-hour test.

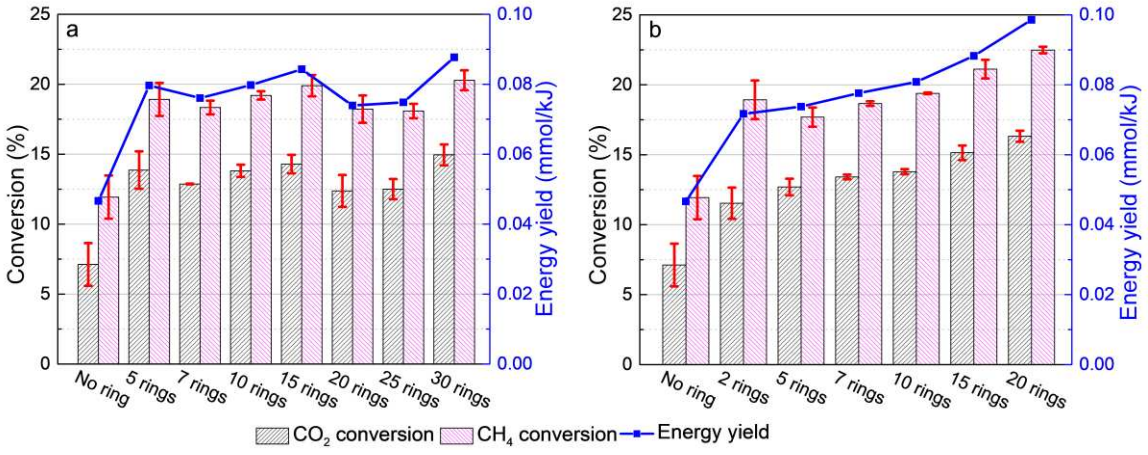

Fig. 8. CH_4 and CO_2 conversion and energy yield of plasma-based dry reforming at 30 W supplied power, in a DBD reactor without rings, and with varying number of stainless steel rings with cross-sectional diameters of (a) 1.6 mm and (b) 3.2 mm. The error bars were obtained from standard errors based on three repeat experiments with the rings kept in place.

The effects of adding the stainless steel rings on the discharge has been described in section 3.1 above, and also apply here, i.e., a higher displaced charge, a larger discharge fraction, a higher discharge intensity, etc. In addition, the discharge in the reactor without rings is unstable at 30 W supplied power (see section 3.2.2 below), which is one of the reasons that the improvement of the reactor performance by the metal rings is so large at 30 W. On the other hand, the positive effects of the metal rings on the discharge is indeed greater at 30 W supplied power, as can be deduced below from the larger changes in parameters such as the discharge fraction and burning voltage.

3.2.2. Electrical characterization

Table 3 shows the collected and calculated electrical characterization data of the experiments in Fig. 8, to better understand the effect of the stainless steel rings at 30 W supplied power. Similar to the case of 50 W, in most cases, the required applied V_{RMS} to achieve a 30 W supplied power in the reactors with rings is smaller than in the reactor without rings. The required V_{RMS} decreases with the number of rings, while the I_{RMS} of the generated plasma increase. The rings in the reactor promoted the generation of discharges and led to more or stronger discharges. The trend of V_{RMS} and I_{RMS} of the reactors with 1.6 mm rings is not obvious when the number of rings is more than 10. For the 3.2 mm rings, the V_{RMS} is lower and the I_{RMS} was higher than for the same number of 1.6 mm rings, and the trend of V_{RMS} with the number of rings was again more pronounced. Thicker rings also have a more pronounced improvement on the discharge. However, different from the

experiments at 50 W supplied power, the generated plasma power in all the reactors with rings is higher than in the reactor without rings. This is because the plasma in the reactor without rings is unstable, extinguishing or not discharging for some periods. As shown in Fig. S5 in the SI, in 6 periods of 2 ms, there was no discharge in 4 half periods. This is also one of the reasons for the poor performance of the reactor without rings at 30 W supplied power. Since the plasma power is calculated as the average power over all periods, including the phases without discharge, the plasma power in the reactor without rings is lower than in the other reactors.

Table 3. Measured data from the input signals of the oscilloscope, including voltage, current, charge and power, for the DBD reactors without rings and with stainless steel rings of varying number and two different cross-sectional diameters, at an almost constant supplied power of 30 W.

Cross-sectional diameter of rings	Number of rings	V_{RMS} (kV)	I_{RMS} plasma (mA)	Plasma power (W)	Supplied power (W)	Displaced charge (nC/period)
Without rings	0	7.42 ± 0.07	14.4 ± 0.6	10.2 ± 0.6	30.4 ± 0.9	360 ± 21
1.6 mm	5	6.33 ± 0.04	13.9 ± 0.4	16.4 ± 0.6	30.6 ± 0.5	700 ± 7
	7	5.99 ± 0.04	14.6 ± 0.3	16.0 ± 0.4	30.5 ± 0.5	718 ± 6
	10	5.69 ± 0.04	17.2 ± 0.7	18.0 ± 0.3	30.8 ± 0.6	780 ± 13
	15	5.51 ± 0.07	16.6 ± 0.5	17.3 ± 0.6	30.2 ± 0.3	770 ± 11
	20	5.63 ± 0.04	17.7 ± 0.3	17.4 ± 0.7	30.8 ± 0.8	790 ± 11
	25	5.66 ± 0.02	17.5 ± 0.3	16.6 ± 0.5	30.4 ± 0.4	766 ± 5
	30	5.62 ± 0.04	17.8 ± 0.2	16.1 ± 0.4	29.9 ± 0.5	734 ± 7
3.2 mm	2	6.89 ± 0.11	15.6 ± 0.3	14.2 ± 0.9	31.6 ± 0.7	700 ± 16
	5	5.87 ± 0.01	16.4 ± 0.7	15.4 ± 0.3	30.7 ± 0.8	850 ± 13
	7	5.55 ± 0.04	17.2 ± 0.5	15.4 ± 0.7	30.8 ± 0.5	884 ± 9
	10	5.30 ± 0.02	18.2 ± 0.8	15.7 ± 0.3	30.5 ± 0.4	930 ± 4
	15	5.06 ± 0.04	19.1 ± 0.4	15.9 ± 0.3	30.6 ± 0.4	1000 ± 12
	20	5.04 ± 0.02	19.4 ± 0.3	15.3 ± 0.5	30.2 ± 0.5	990 ± 11

Fig. 9 shows the fitted Lissajous figures of the plasma at 30 W supplied power, in the reactors without rings and with varying number and two different cross-sectional diameter of the stainless steel rings. The raw data of the Lissajous figures are shown in Fig. S6. It should be noted that the Lissajous figure of the reactor without rings is only in the discharge phases, because the Lissajous figure could not be formed in the undischarged period. The Lissajous figures at 30 W exhibit more obvious differences between the reactors with and without rings than at 50 W supplied power. First of all, the height of the Lissajous figures, reflecting the displaced charge (see Table 3), follows the same trend, which is higher for the reactors with rings than for the reactor without rings, and increases with the number of rings. After placing a certain number of rings (e.g. 15 of 1.6 mm rings), a larger number of rings does not enhance the displaced charge anymore. The enhancement of displaced charge by the rings is more than double or even nearly triple that of the reactor without rings, indicating that the promotion of stainless steel rings on the plasma is greater at 30 W. Furthermore, the displaced charge of the 3.2 mm rings was also more than that of the 1.6 mm rings with the same number of rings at 30 W, so the reactors with 3.2 mm rings also yield a higher performance. Second, the U_{bur} reflecting the voltage for igniting and sustaining the plasma, calculated from the Lissajous figures, was reduced by the metal rings, in a similar trend as at 50 W. At 30 W supplied power, the mean electric field and the mean electron energy also follow similar trends to those at 50 W, and even have similar values. They increase with the increase of the cross-sectional diameter of the rings, and decrease upon larger number of rings. The electron energy distribution function is shown in Fig. S7. Despite the similar values for electric field and mean electron energy for the reactor configurations with rings at 50 W and 30 W, the reactor without rings has higher values for the burning voltage, average electric field, and electron energy at 30 W than 50 W, probably due to the unstable discharge at low power, which could be one of the reasons for its poor performance at 30 W. At 30 W, the burning voltage in the reactors with rings is smaller than in the reactor without rings, and the mean electric field and mean electron energy as well, for the 1.6 mm rings, while it is higher for the 3.2 mm rings. In spite of this, the performance of the

reactors with rings is always better at 30 W than for the reactor without rings. Finally, the capacitance of different phases of the DBD reactor, C_{cell} and ζ, calculated from the slope of the Lissajous figures, are listed in Table 4, as well as the discharge fractions, which are also calculated from them. The tendency of capacitance and discharge fraction due to the presence of the rings is the same as at 50 W. Thicker and more rings increase the capacitance and the discharge fraction. The 1.6 mm rings increase the discharge fraction from 30.0% for 5 rings to 44.7% for 30 rings, while the 3.2 mm rings increase the discharge fraction from 20.1% for 2 rings to 51.4% for 20 rings, with a larger increase rate. The discharge fraction of the reactors with relatively few (≤ 5) rings were smaller than that of the reactor without rings, probably because the rings induce the discharge to mainly take place on them, as mentioned above in section 3.1.2. The discharge fraction of the same reactor at 30 W was less than at 50 W. However, compared with the ring-free reactor, some plasma parameters, including the discharge fraction, burning voltage and displaced charge, were improved more by the presence of rings at 30W than at 50W, which is another reason why the reactor with stainless steel rings showed better performance at 30W.

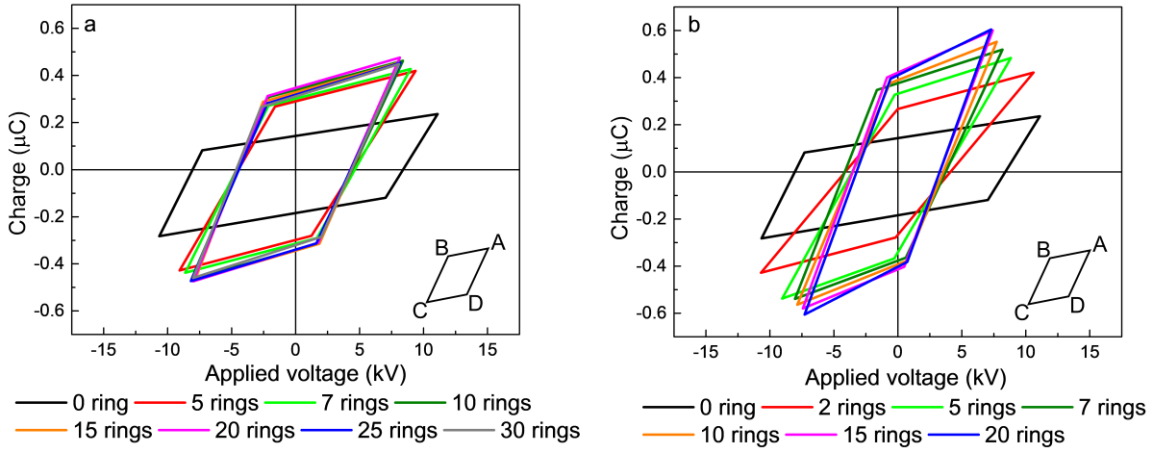

Fig. 9. The fitted Lissajous figures (calculated by the MATLAB script) of plasma-based dry reforming at 30 W supplied power, in a DBD reactor without rings and with varying number of stainless steel rings with cross-sectional diameters of (a) 1.6 mm and (b) 3.2 mm.

Table 4. Calculated data derived from the raw data of electrical characterization, obtained by a MATLAB script and BOLSIG+, for the DBD reactors without rings and with stainless steel rings of varying number and two different cross-sectional diameters, at an almost constant supplied power of 30 W.

Cross-sectional diameter of rings	Number of rings	U_{bur} (kV)	Electric field (kV/cm)	Mean electron energy (eV)	C_{cell} (pF)	ζ (pF)	f (%)	Number of micro-discharges (a.u./T)	Average filament charge (nC/disch.)
Without rings	0	8.9 ± 0.3	18.1 ± 0.6	4.05 ± 0.07	8.8 ± 0.7	98.0 ± 0.5	34.7 ± 0.3	68 ± 9	5 ± 2
1.6 mm	5	5.1 ± 0.2	15.4 ± 0.6	3.71 ± 0.07	14.0 ± 0.5	89.7 ± 0.7	30.0 ± 0.3	97 ± 2	7 ± 1
	7	5.08 ± 0.07	15.3 ± 0.2	3.70 ± 0.06	14.2 ± 0.8	103.5 ± 0.4	35.5 ± 0.4	139 ± 4	5 ± 1
	10	4.8 ± 0.1	14.5 ± 0.3	3.58 ± 0.06	15.0 ± 0.8	122.6 ± 0.7	42.8 ± 0.2	110 ± 12	7 ± 3
	15	4.7 ± 0.1	14.2 ± 0.3	3.53 ± 0.06	16 ± 0.1	133.4 ± 0.9	47.0 ± 0.1	92 ± 6	8 ± 2
	20	4.6 ± 0.2	13.9 ± 0.6	3.48 ± 0.07	16.3 ± 0.4	129 ± 1	45.2 ± 0.4	99 ± 3	8 ± 2
	25	4.67 ± 0.05	14.1 ± 0.2	3.52 ± 0.06	16.4 ± 0.9	121.5 ± 0.3	42.1 ± 0.4	101 ± 7	8 ± 3
	30	4.7 ± 0.2	14.2 ± 0.6	3.53 ± 0.07	17.2 ± 0.4	128.5 ± 0.9	44.7 ± 0.4	117 ± 2	6 ± 2
3.2 mm	2	5.0 ± 0.2	29.2 ± 1.2	5.09 ± 0.12	14.4 ± 0.8	65.0 ± 0.4	20.1 ± 0.3	71 ± 3	10 ± 2
	5	4.2 ± 0.1	24.5 ± 0.6	4.70 ± 0.07	18.3 ± 0.6	95.9 ± 0.2	31.3 ± 0.3	107 ± 6	8 ± 3
	7	4.08 ± 0.04	23.8 ± 0.2	4.64 ± 0.06	18.8 ± 0.5	127.8 ± 0.7	44.1 ± 0.2	161 ± 4	6 ± 2
	10	3.9 ± 0.1	22.8 ± 0.6	4.54 ± 0.07	21.5 ± 0.7	131.2 ± 0.6	44.9 ± 0.1	135 ± 5	7 ± 1
	15	3.6 ± 0.1	21.0 ± 0.6	4.37 ± 0.07	23.3 ± 0.4	147.1 ± 0.4	51.0 ± 0.1	101 ± 5	10 ± 1
	20	3.6 ± 0.1	21.0 ± 0.6	4.37 ± 0.07	27.2 ± 0.4	149.9 ± 0.8	51.4 ± 0.3	124 ± 3	8 ± 2

Fig. 10 shows the current profiles in the DBD reactors at 30 W supplied power. It should be noted that the current profile of the reactor without rings is selected from the stable discharge phases,

and actually it is not discharged in some phases, as shown in Fig. S5. At 30 W supplied power, the stainless steel rings are again able to make the discharge more uniform in intensity, even with only 2 or 5 rings. As the number of rings increases, the uniformity of the current intensity of the plasma decreases slightly, see for example the reactors with 5 and 20 rings with a diameter of 3.2 mm. The onset of the discharge was earlier in the reactors with rings due to the reduction in U_{bur}. The number of micro-discharges and average filament charge were calculated and listed in Table 4. Different from the experiments at 50 W, where the 1.6 mm rings or 3.2 mm rings can only increase either the average filament charge or the number of micro-discharges, at 30 W supplied power, both these parameters are higher in the reactors with rings than in the reactor without rings. The reason for the larger number of micro-discharges by the rings with both diameters is that the discharge in the reactor without rings at 30 W is unstable and extinguishes in some periods. Moreover, with a larger number of micro-discharges, the average displaced charge per discharge of the reactor with rings is still higher than that of the reactor without rings. This indicates again that at 30 W supplied power, the improvement of the discharge by the metal rings is greater than that at 50 W.

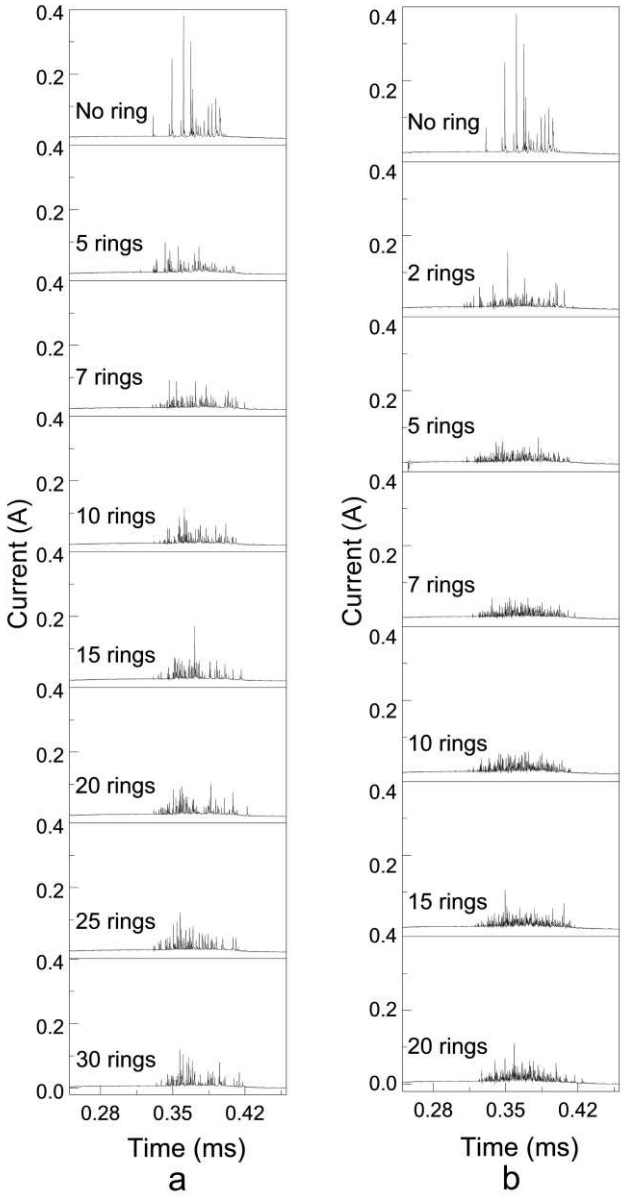

Fig. 10. Current profiles of a discharge phase in DBD reactors at 30 W supplied power, for the reactor without rings and with varying number of stainless steel rings with cross-sectional diameters of (a) 1.6 mm and (b) 3.2 mm.

3.2.3. Selectivity

Fig. 11 shows the selectivity of syngas and various by-products of the plasma-based dry reforming in the DBD reactors with stainless steel rings at 30 W supplied power. In most cases, the syngas selectivity in the reactors with rings is slightly higher than in the reactor without rings. In fact, the higher selectivity resulting from the rings seems to be present at 50 W as well, but is less obvious. Fig. S8 shows the carbon and hydrogen atomic balance, plotted from Fig. 11, and the atomic balance of the reactor with rings is higher than for the reactor without rings. This may be due to the fact that the products of plasma-based dry reforming were formed by the reaction of various radicals generated by the discharge, and the more uniform intensity of the discharge could reduce the types of formed by-products [26].

In addition, lower power seems to be favorable for improving the selectivity of some products. The selectivity of CO, H_2, ethylene, acetylene, methanol, and ethanol at 30 W was higher than at 50 W, while the selectivity of other products was not much different. Close observation and comparison of the selectivity at 30 W and 50 W shows similarities in the trend of selectivity of some products at different powers. This also proves that although there are mainly physical effects, the stainless steel rings can have a certain effect on the product selectivity as well.

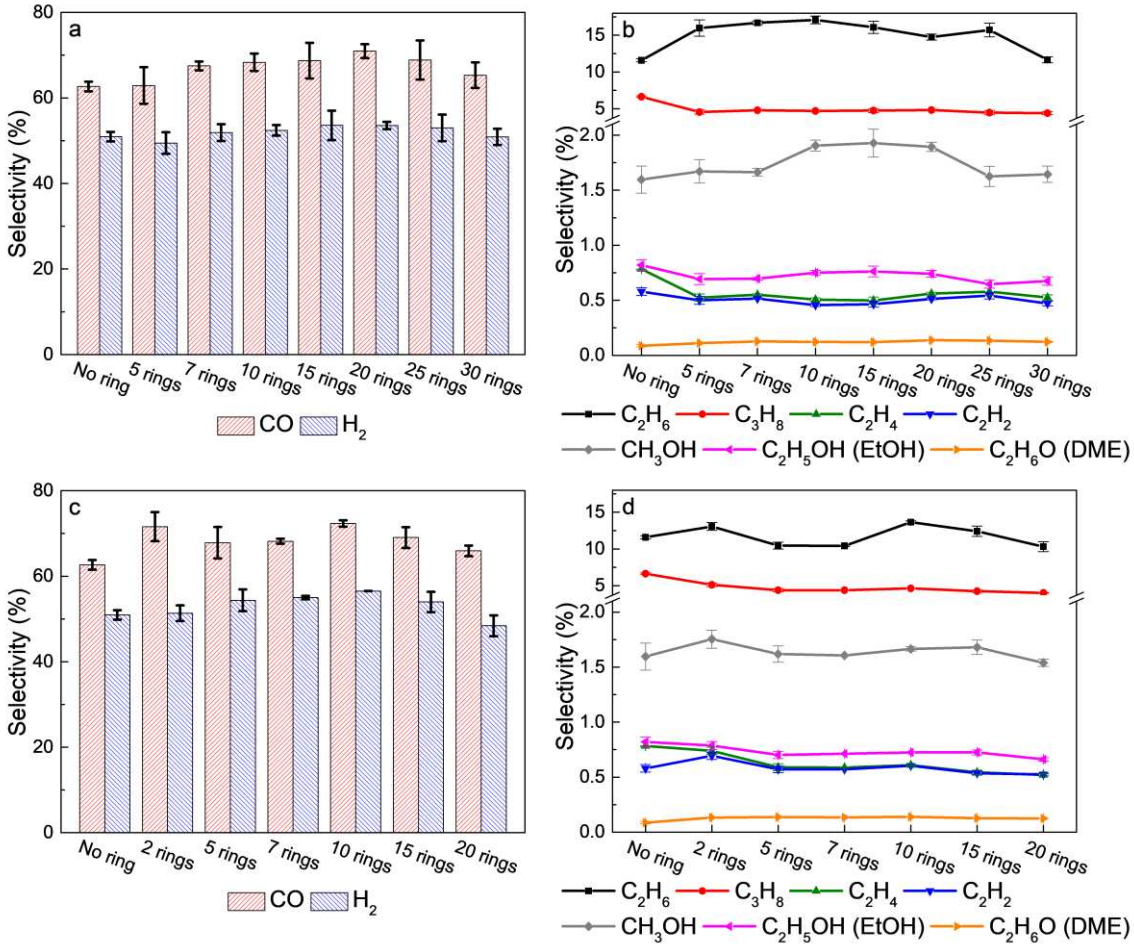

Fig. 11. Selectivity of various products of plasma-based dry reforming at 30 W supplied power, in a DBD reactor without rings and with varying number of stainless steel rings. (a) Syngas and (b) ethane, propane, ethylene, acetylene, methanol, ethanol (EtOH) and dimethyl ether (DME) selectivity in reactors with rings with a diameter of 1.6 mm. (c) Syngas and (d) ethane, propane, ethylene, acetylene, methanol, ethanol and dimethyl ether selectivity in reactors with rings with a diameter of 3.2 mm. The error bars were obtained from standard errors based on three repeat experiments with the rings kept in place.

3.3. Advantages of the reactor with rings

Due to different operating conditions (i.e., various gas composition and discharge parameters), it is difficult to accurately compare the reactor performance with literature. However, when we roughly compare the energy yields in literature (~0.1 mmol/kJ in empty reactors and ~0.2 mmol/kJ in reactors with catalyst) [4,7,23], the energy yield of 0.19 mmol/kJ achieved in our reactor configuration with rings but in absence of packing materials or catalyst, as obtained in this work, can be considered to be competitive. In addition, a lower power is generally favorable for higher

energy yield and higher liquefiable products selectivity, as demonstrated in this work and in the literature [7,36]. However, it is difficult to stabilize the discharge at lower power in the original reactor without rings. Therefore, another advantage of a reactor configuration with rings is to help stabilize the discharge at lower power.

In addition to the above dry reforming processes, and in order to verify whether the DBD reactor with rings can also be applied to other plasma-based reactions, we performed experiments for CO_2 decomposition at 30 W in the reactor with and without 3.2 mm rings. As shown in Fig. S9, the conversion of CO_2 in the reactor with rings is again higher than in the reactor without rings, indicating that this DBD reactor design has the potential to be extended to other plasma-based processes. More in-depth research and analysis on CO_2 decomposition and other processes could be the subject of future work, to get more insights in the underlying mechanisms.

4 Conclusion

In this study, we put stainless steel rings over the inner electrode rod of a cylindrical DBD reactor, to change the local discharge gap and the electric field, and to study the dry reforming performance. A varying number of rings with cross-sectional diameters of 1.6 mm and 3.2 mm (leading to 3.1 mm and 1.5 mm discharge gaps) were used, and experiments were carried out at 50 W and 30 W supplied power. We found that at 50 W, the stainless steel rings mainly have negative effects on the performance, while at 30 W, the rings greatly improve the performance, both in terms of reactant conversion and energy yield. The reactor with 20 rings with 3.2 mm diameter showed the best performance. Compared to the reactor without rings, it increases the CO_2 conversion from 7.1% to 16.3 %, the CH_4 conversion from 11.9% to 22.5%, and the energy yield from 0.05 mmol/kJ to 0.10 mmol/kJ (0.19 mmol/kJ if it was calculated from the plasma power). All reactors with rings have higher energy yield at 30 W than at 50 W.

Since the rings are made of similar material as the inner electrode and with small surface area, we believe that the rings mainly cause physical effects on the discharge, and catalytic effects are not considered. The difference in performance caused by the rings can be understood from studying the electrical characteristics. The presence of the stainless steel rings changes the electric field distribution in the reactor. The discharge gap is smaller where the rings are placed, increasing the local electric field. Through electrical characterization, it was found that the displaced charge and the discharge fraction, which can improve the conversion and energy yield of plasma-based dry reforming, increase with the number and the cross-sectional diameter of rings at the same energy input. This is the reason that the 3.2 mm rings always exhibit higher performance than the 1.6 mm rings. The non-uniform discharge gap caused by the rings makes the discharge more stable and more uniform in intensity, although its spatial distribution may be non-uniform. This spatial non-uniformity was reduced by placing more rings, while the positive effects such as displaced charge were enhanced, leading to better performance in reactors with more rings. At 30 W supplied power, the metal rings can stabilize the discharge and have a greater improvement in the discharge than at 50 W, and thus yield better performance. Moreover, the effect of the stainless steel rings on the discharge can also alter the selectivity of some products. The largest impact on selectivity is however caused by lowering the supplied plasma power to 30W, increasing the selectivity of e.g. methanol and ethane.

Besides dry reforming, the performance differences by placing metal rings in the DBD reactor to alter the discharge gap distribution may be applicable to other plasma-based processes as well. In addition, in plasma catalysis, the metal active components on the catalyst surface can also change the discharge gap and electric field distribution in the reactor, and the effects mentioned above might also play some role there. Catalyst studies to improve the conversion and selectivity of

plasma reactions need to consider not only its catalytic activity, but also these effects on the discharge behavior.

Declaration of competing interest

The authors declare no known competing financial interest or personal relationships that could inappropriately influence this work.

Acknowledgements

J.W acknowledges the financial support from the China Scholarship Council (No. 201806060123). K.Z acknowledges the EASiCHEM project funded by the Flemish Strategic Basic Research Program of the Catalisti cluster and Flanders Innovation & Entrepreneurship (HBC.2018.0484).

Appendix A. Supporting information

Supplementary data associated with this article can be found in the online version.

References

[1] A. Bogaerts, X. Tu, J.C. Whitehead, G. Centi, L. Lefferts, O. Guaitella, F. Azzolina-Jury, H.-H. Kim, A.B. Murphy, W.F. Schneider, T. Nozaki, J.C. Hicks, A. Rousseau, F. Thevenet, A. Khacef, M. Carreon, The 2020 plasma catalysis roadmap, J. Phys. D Appl. Phys. 53 (2020) 443001. https://doi.org/10.1088/1361-6463/ab9048.

[2] Y. Yi, J. Zhou, H. Guo, J. Zhao, J. Su, L. Wang, X. Wang, W. Gong, Safe Direct Synthesis of High Purity H_2O_2 through a H_2/O_2 Plasma Reaction, Angew. Chem. Int. Ed. 52 (2013) 8446-8449. https://doi.org/https://doi.org/10.1002/anie.201304134.

[3] Y. Yi, S. Li, Z. Cui, Y. Hao, Y. Zhang, L. Wang, P. Liu, X. Tu, X. Xu, H. Guo, A. Bogaerts, Selective oxidation of CH_4 to CH_3OH through plasma catalysis: Insights from catalyst characterization and chemical kinetics modelling, Appl. Catal. B Environ. 296 (2021) 120384. https://doi.org/10.1016/j.apcatb.2021.120384.

[4] A.H. Khoja, M. Tahir, N.A.S. Amin, Dry reforming of methane using different dielectric materials and DBD plasma reactor configurations, Energy Convers. Manage. 144 (2017) 262-274. https://doi.org/https://doi.org/10.1016/j.enconman.2017.04.057.

[5] Y. Uytdenhouwen, J. Hereijgers, T. Breugelmans, P. Cool, A. Bogaerts, How gas flow design can influence the performance of a DBD plasma reactor for dry reforming of methane, Chem. Eng. J. 405 (2021) 126618. https://doi.org/https://doi.org/10.1016/j.cej.2020.126618.

[6] S. Zhang, Y. Gao, H. Sun, Z. Fan, T. Shao, Dry reforming of methane by microsecond pulsed dielectric barrier discharge plasma: Optimizing the reactor structures, High Voltage 7 (2022) 718-729. https://doi.org/https://doi.org/10.1049/hve2.12201.

[7] C.-j. Liu, G.-h. Xu, T. Wang, Non-thermal plasma approaches in CO_2 utilization, Fuel Process. Technol. 58 (1999) 119-134. https://doi.org/https://doi.org/10.1016/S0378-3820(98)00091-5.

[8] X. Tu, J.C. Whitehead, Plasma-catalytic dry reforming of methane in an atmospheric dielectric barrier discharge: Understanding the synergistic effect at low temperature, Appl. Catal. B Environ. 125 (2012) 439-448. https://doi.org/https://doi.org/10.1016/j.apcatb.2012.06.006.

[9] R. Snoeckx, A. Bogaerts, Plasma technology – a novel solution for CO_2 conversion?, Chem. Soc. Rev. 46 (2017) 5805-5863. https://doi.org/10.1039/C6CS00066E.

[10] B.S. Patil, N. Cherkasov, J. Lang, A.O. Ibhadon, V. Hessel, Q. Wang, Low temperature plasma-catalytic NO_x synthesis in a packed DBD reactor: Effect of support materials and supported active metal oxides, Appl. Catal. B Environ. 194 (2016) 123-133. https://doi.org/10.1016/j.apcatb.2016.04.055.
[11] L. Wang, Y. Yi, C. Wu, H. Guo, X. Tu, One-Step Reforming of CO_2 and CH_4 into High-Value Liquid Chemicals and Fuels at Room Temperature by Plasma-Driven Catalysis, Angew. Chem. Int. Ed. 56 (2017) 13679-13683. https://doi.org/https://doi.org/10.1002/anie.201707131.
[12] Y. Uytdenhouwen, K.M. Bal, E.C. Neyts, V. Meynen, P. Cool, A. Bogaerts, On the kinetics and equilibria of plasma-based dry reforming of methane, Chem. Eng. J. 405 (2021) 126630. https://doi.org/https://doi.org/10.1016/j.cej.2020.126630.
[13] X. Tu, J.C. Whitehead, Plasma dry reforming of methane in an atmospheric pressure AC gliding arc discharge: Co-generation of syngas and carbon nanomaterials, Int. J. Hydrogen Energy 39 (2014) 9658-9669. https://doi.org/https://doi.org/10.1016/j.ijhydene.2014.04.073.
[14] Y. Yi, C. Xu, L. Wang, J. Yu, Q. Zhu, S. Sun, X. Tu, C. Meng, J. Zhang, H. Guo, Selectivity control of H_2/O_2 plasma reaction for direct synthesis of high purity H_2O_2 with desired concentration, Chem. Eng. J. 313 (2017) 37-46. https://doi.org/https://doi.org/10.1016/j.cej.2016.12.043.
[15] Y. Yi, X. Wang, A. Jafarzadeh, L. Wang, P. Liu, B. He, J. Yan, R. Zhang, H. Zhang, X. Liu, H. Guo, E.C. Neyts, A. Bogaerts, Plasma-Catalytic Ammonia Reforming of Methane over Cu-Based Catalysts for the Production of HCN and H_2 at Reduced Temperature, ACS Catalysis 11 (2021) 1765-1773. https://doi.org/10.1021/acscatal.0c04940.
[16] X. Gao, Z. Lin, T. Li, L. Huang, J. Zhang, S. Askari, N. Dewangan, A. Jangam, S. Kawi, Recent Developments in Dielectric Barrier Discharge Plasma-Assisted Catalytic Dry Reforming of Methane over Ni-Based Catalysts, Catalysts 11 (2021). https://doi.org/10.3390/catal11040455.
[17] R. Vakili, R. Gholami, C.E. Stere, S. Chansai, H. Chen, S.M. Holmes, Y. Jiao, C. Hardacre, X. Fan, Plasma-assisted catalytic dry reforming of methane (DRM) over metal-organic frameworks (MOFs)-based catalysts, Appl. Catal. B Environ. 260 (2020) 118195. https://doi.org/https://doi.org/10.1016/j.apcatb.2019.118195.
[18] W.-C. Chung, M.-B. Chang, Review of catalysis and plasma performance on dry reforming of CH_4 and possible synergistic effects, Renewable and Sustainable Energy Reviews 62 (2016) 13-31. https://doi.org/https://doi.org/10.1016/j.rser.2016.04.007.
[19] A.H. Khoja, M. Tahir, N.A.S. Amin, Recent developments in non-thermal catalytic DBD plasma reactor for dry reforming of methane, Energy Convers. Manage. 183 (2019) 529-560. https://doi.org/https://doi.org/10.1016/j.enconman.2018.12.112.
[20] A. Ozkan, T. Dufour, A. Bogaerts, F. Reniers, How do the barrier thickness and dielectric material influence the filamentary mode and CO_2 conversion in a flowing DBD?, Plasma Sources Sci. Technol. 25 (2016) 045016. https://doi.org/10.1088/0963-0252/25/4/045016.
[21] A. Ozkan, T. Dufour, T. Silva, N. Britun, R. Snyders, A. Bogaerts, F. Reniers, The influence of power and frequency on the filamentary behavior of a flowing DBD—application to the splitting of CO_2, Plasma Sources Sci. Technol. 25 (2016) 025013. https://doi.org/10.1088/0963-0252/25/2/025013.
[22] P. Vanraes, A. Nikiforov, A. Bogaerts, C. Leys, Study of an AC dielectric barrier single micro-discharge filament over a water film, Scientific Reports 8 (2018) 10919. https://doi.org/10.1038/s41598-018-29189-w.
[23] K. van 't Veer, Y. Engelmann, F. Reniers, A. Bogaerts, Plasma-Catalytic Ammonia Synthesis in a DBD Plasma: Role of Microdischarges and Their Afterglows, J. Phys. Chem. C 124 (2020) 22871-22883. https://doi.org/10.1021/acs.jpcc.0c05110.
[24] C. De Bie, J. van Dijk, A. Bogaerts, The Dominant Pathways for the Conversion of Methane into Oxygenates and Syngas in an Atmospheric Pressure Dielectric Barrier Discharge, J. Phys. Chem. C 119 (2015) 22331-22350. https://doi.org/10.1021/acs.jpcc.5b06515.

[25] R. Snoeckx, R. Aerts, X. Tu, A. Bogaerts, Plasma-Based Dry Reforming: A Computational Study Ranging from the Nanoseconds to Seconds Time Scale, J. Phys. Chem. C 117 (2013) 4957-4970. https://doi.org/10.1021/jp311912b.
[26] D. Ray, P.M.K. Reddy, C. Subrahmanyam, Ni-Mn/γ-Al_2O_3 assisted plasma dry reforming of methane, Catal. Today 309 (2018) 212-218. https://doi.org/https://doi.org/10.1016/j.cattod.2017.07.003.
[27] A. Bogaerts, G. Centi, Plasma technology for CO_2 conversion: a personal perspective on prospects and gaps, Frontiers in Energy Research 8 (2020) 111.
[28] A. Ağıral, T. Nozaki, M. Nakase, S. Yuzawa, K. Okazaki, J.G.E. Gardeniers, Gas-to-liquids process using multi-phase flow, non-thermal plasma microreactor, Chem. Eng. J. 167 (2011) 560-566. https://doi.org/https://doi.org/10.1016/j.cej.2010.10.050.
[29] H. Sekiguchi, M. Ando, H. Kojima, Study of hydroxylation of benzene and toluene using a micro-DBD plasma reactor, J. Phys. D Appl. Phys. 38 (2005) 1722-1727. https://doi.org/10.1088/0022-3727/38/11/013.
[30] Y. Uytdenhouwen, S. Van Alphen, I. Michielsen, V. Meynen, P. Cool, A. Bogaerts, A packed-bed DBD micro plasma reactor for CO_2 dissociation: Does size matter?, Chem. Eng. J. 348 (2018) 557-568. https://doi.org/https://doi.org/10.1016/j.cej.2018.04.210.
[31] Y. Uytdenhouwen, K.M. Bal, I. Michielsen, E.C. Neyts, V. Meynen, P. Cool, A. Bogaerts, How process parameters and packing materials tune chemical equilibrium and kinetics in plasma-based CO_2 conversion, Chem. Eng. J. 372 (2019) 1253-1264. https://doi.org/https://doi.org/10.1016/j.cej.2019.05.008.
[32] N. Pinhão, A. Moura, J.B. Branco, J. Neves, Influence of gas expansion on process parameters in non-thermal plasma plug-flow reactors: A study applied to dry reforming of methane, Int. J. Hydrogen Energy 41 (2016) 9245-9255. https://doi.org/https://doi.org/10.1016/j.ijhydene.2016.04.148.
[33] W.-C. Chung, K.-L. Pan, H.-M. Lee, M.-B. Chang, Dry Reforming of Methane with Dielectric Barrier Discharge and Ferroelectric Packed-Bed Reactors, Energy & Fuels 28 (2014) 7621-7631. https://doi.org/10.1021/ef5020555.
[34] F.J.J. Peeters, M.C.M. van de Sanden, The influence of partial surface discharging on the electrical characterization of DBDs, Plasma Sources Sci. Technol. 24 (2014) 015016. https://doi.org/10.1088/0963-0252/24/1/015016.
[35] Y. Wang, Y. Chen, J. Harding, H. He, A. Bogaerts, X. Tu, Catalyst-free single-step plasma reforming of CH_4 and CO_2 to higher value oxygenates under ambient conditions, Chem. Eng. J. 450 (2022) 137860. https://doi.org/https://doi.org/10.1016/j.cej.2022.137860.
[36] G.J.M. Hagelaar, L.C. Pitchford, Solving the Boltzmann equation to obtain electron transport coefficients and rate coefficients for fluid models, Plasma Sources Sci. Technol. 14 (2005) 722. https://doi.org/10.1088/0963-0252/14/4/011.
[37] K. van ‘t Veer, S. van Alphen, A. Remy, Y. Gorbanev, N. De Geyter, R. Snyders, F. Reniers, A. Bogaerts, Spatially and temporally non-uniform plasmas: microdischarges from the perspective of molecules in a packed bed plasma reactor, J. Phys. D Appl. Phys. 54 (2021) 174002. https://doi.org/10.1088/1361-6463/abe15b.
[38] R. Aerts, W. Somers, A. Bogaerts, Carbon Dioxide Splitting in a Dielectric Barrier Discharge Plasma: A Combined Experimental and Computational Study, ChemSusChem 8 (2015) 702-716. https://doi.org/https://doi.org/10.1002/cssc.201402818.
[39] B. Wang, W. Yan, W. Ge, X. Duan, Kinetic model of the methane conversion into higher hydrocarbons with a dielectric barrier discharge microplasma reactor, Chem. Eng. J. 234 (2013) 354-360. https://doi.org/https://doi.org/10.1016/j.cej.2013.08.052.